ESC European Society of Cardiology

European Heart Journal (2021) **42**, 740–749
doi:10.1093/eurheartj/ehaa1035

SPECIAL ARTICLE

The year in cardiovascular medicine 2020: imaging

José Luis Zamorano[1]*, Fausto J. Pinto [2], Jorge Solano-López[1], and Chiara Bucciarelli-Ducci[3]

[1]Department of Cardiology, University Hospital Ramon y Cajal, Carretera de Colmenar Km 9.100, 28034 Madrid; Spain; [2]Department of Cardiology, Centro Hospitalar Universitário Lisboa Norte (CHULN), CCUL, Universidade de Lisboa, Av. Prof. Egas Moniz MB 1649-028 Lisboa, Portugal; and [3]Department of Cardiology, Bristol Heart Institute, University Hospitals Bristol and Weston NHS Trust and University of Bristol, UK

Received 9 October 2020; revised 13 November 2020; editorial decision 3 December 2020; accepted 7 December 2020; online publish-ahead-of-print 3 January 2021

Graphical Abstract

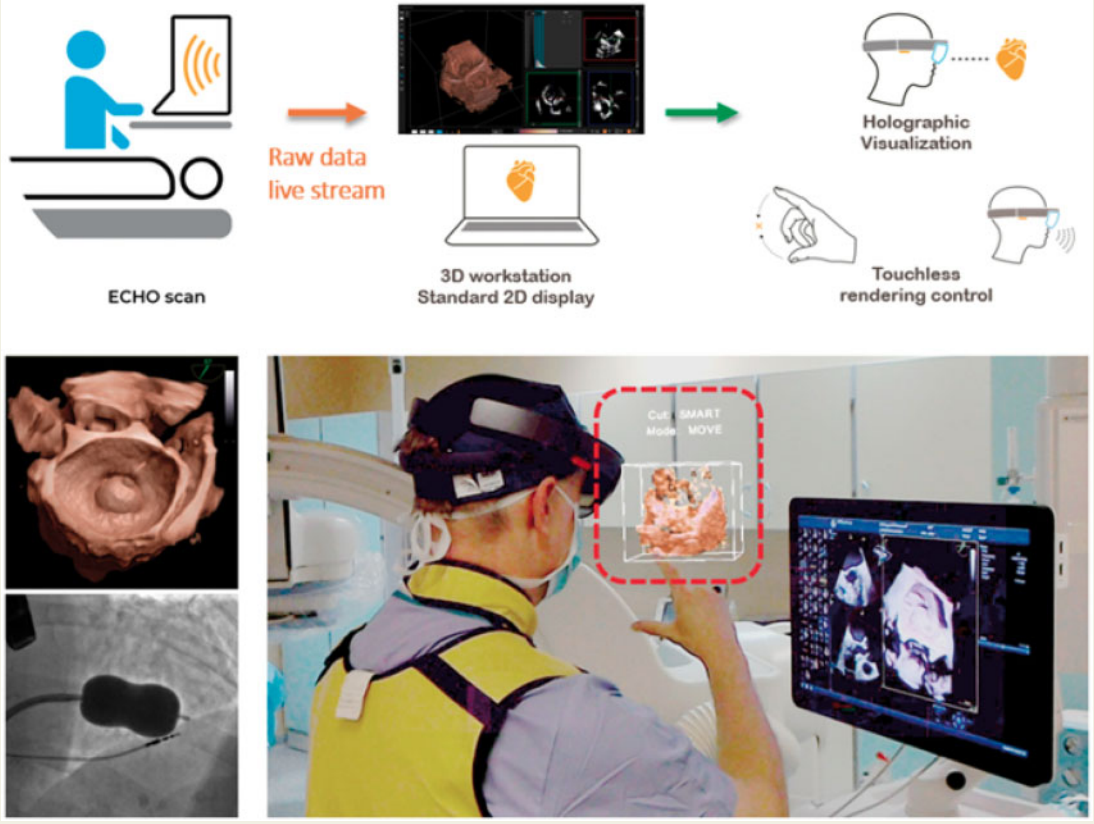

Raw 3D data were streamed from standard echocardiograph using custom connection to 3D DICOM viewer workstation (CarnaLife Holo, MedApp, Krakow, Poland) for real-time, dynamic 3D rendering and wirelessly transferred into HoloLens mixed reality display (Microsoft, Redmond, USA) to overlay non-obstructive 3D data hologram upon reality view. Data were visible as a semitransparent holographic cube positioned in a convenient sector of visual field of echocardiographist and shared by interventional cardiologist. Reproduced with permission from Kasprzak *et al.*[7]

* Corresponding author. Tel: +34 913368515; Email: zamorano@secardiologia.es

Keywords Echocardiography • CT scan • Cardiac magnetic resonance • Nuclear cardiology

Introduction

The past year has been a unique one owing to the outbreak of COVID-19, which has affected the population worldwide, with the ensuing economic and social consequences. The field of cardiology has not escaped this reality bringing with it changes in our everyday clinical praxis. The contribution of different imaging techniques to the cardiac involvement of COVID-19 with diagnostic and prognostic implications has been published very expeditiously. It is still pending to ascertain the long-term outcome of the different degrees of cardiac injury.

The recent publication of the ISCHEMIA trial[1] has resulted in a heated debate on the role of ischaemia testing in patients with stable coronary artery disease (CAD), with some colleagues advocating that ISCHEMIA has sanctioned the limited role of myocardial ischaemia in patients with stable CAD. However, this is not the conclusion of the trial, nor its primary hypothesis nor the study design and extrapolation beyond these boundaries could be incorrect. Ischaemia imaging will continue to play a major role in the diagnosis and management of stable CAD as both physicians and patients still need to clarify the cause of symptoms, coronary anatomy does not infer ischaemia or explains symptoms, and chest pain can also be of non-coronary origin. Most importantly, there is no randomized trial demonstrating that an imaging approach of coronary anatomy is superior to functional testing. In fact, PROMISE[2] is the only trial that compared the two strategies and it did not demonstrate any difference in outcome between the two approaches.

Furthermore, advances in the knowledge and application of artificial intelligence (AI) are consolidating the need for greater attention and interest regarding a tool that in a few years will become part of our daily clinical practice. Finally, we highlight the introduction of new recommendations in the use of imaging techniques in the new practice guidelines.

We then summarize the most outstanding studies from the last year relating to the most relevant imaging techniques in current cardiology.

Echocardiography

Echocardiography continues to be one of the most used methods to better understand cardiac pathophysiology and different pathological and even normal aspects of cardiac function and also plays a central role in daily patient management. Several papers have been published in 2020, and here, we highlight just a small proportion of the large amount of literature that has been produced during this year, a very unusual one, considering the COVID-19 pandemic that affected all of us.

One area of great current interest is transthyretin amyloidosis cardiomyopathy (ATTR-CM), an increasingly recognized cause of heart failure (HF) and with the new treatment strategies underway, some already with important clinical results; its recognition is becoming a must in clinical scenarios. Echocardiography has always played a role in the diagnosis of amyloidosis and that role is further strengthened with the exponential increase in relevance of amyloidosis. Chacko *et al.*[3] in an international network characterized the structural and functional echocardiographic phenotype across the spectrum of wild-type (wtATTR-CM) and hereditary (hATTR-CM) transthyretin cardiomyopathy and the echocardiographic features predicting prognosis. They studied 1240 patients with ATTR-CM, comprising 766 with wtATTR-CM and 474 with hATTR-CM, of whom 314 had the V122I variant and 127 the T60A variant. At diagnosis, patients with V122I-hATTR-CM had the most severe degree of systolic and diastolic dysfunction across all echocardiographic parameters and patients with T60A-hATTR-CM the least; patients with wtATTR-CM had intermediate features. Stroke volume index, right atrial area index, longitudinal strain, and E/e' were independently associated with mortality ($P < 0.05$ for all). Severe aortic stenosis (AS) was also independently associated with prognosis, conferring a significantly shorter survival (median survival 22 vs. 53 months, $P = 0.001$). In this study, the three distinct genotypes presented with varying degrees of severity. Echocardiography indicated a complex pathophysiology in which both systolic and diastolic functions were independently associated with mortality. The presence of severe AS was also independently associated with significantly reduced patient survival.

The need for normal values is very important to set the references to determine the pathological boundaries. In this regard, the NORRE study provided useful reference ranges of 2D echocardiographic measurements of left ventricular (LV) layer-specific strain from a large group of healthy volunteers of both genders over a wide range of ages.[4]

The importance of developing parameters that may help the clinician to better understand the severity of certain disease conditions, as well as risk stratify the patients, is of utmost clinical relevance. That is the case of patients with bicuspid aortic valve (BAV). Kong *et al.*,[5] realized a study to evaluate the proportion and prognostic value of impaired LV global longitudinal strain (GLS) in patients with BAV and preserved LV ejection fraction (EF). It evaluated the proportion and prognostic value of impaired LV GLS in patients with BAV and preserved LVEF. Five hundred and thirteen patients with BAV and preserved LVEF (>50%) were divided into five groups according to the type of BAV dysfunction: (i) normal function BAV, (ii) mild AS or aortic regurgitation (AR), (iii) ≥ moderate isolated AS, (iv) ≥ moderate isolated AR, and (v) ≥moderate mixed AS and AR. LV systolic dysfunction based on 2D speckle-tracking echocardiography was defined as a cut-off value of left ventricular global longitudinal strain [LVGLS (-13.6%)]. The primary outcome was aortic valve intervention or all-cause mortality. The proportion of patients with LVGLS ≤-13.6% was the highest in the normal BAV group (97%) and the lowest in the group with moderate and severe mixed AS and AR (79%). During a median follow-up of 10 years, 210 (41%) patients underwent aortic valve replacement and 17 (3%) died. Patients with preserved LV systolic function (LVGLS ≤-13.6%) had significantly better event-free survival compared to those with impaired LV systolic function (LVGLS >-13.6%). LVGLS was independently associated with increased risk of events (mainly aortic valve replacement): hazard ratio (HR) 1.09; $P < 0.001$. Therefore, impaired LVGLS in BAV with

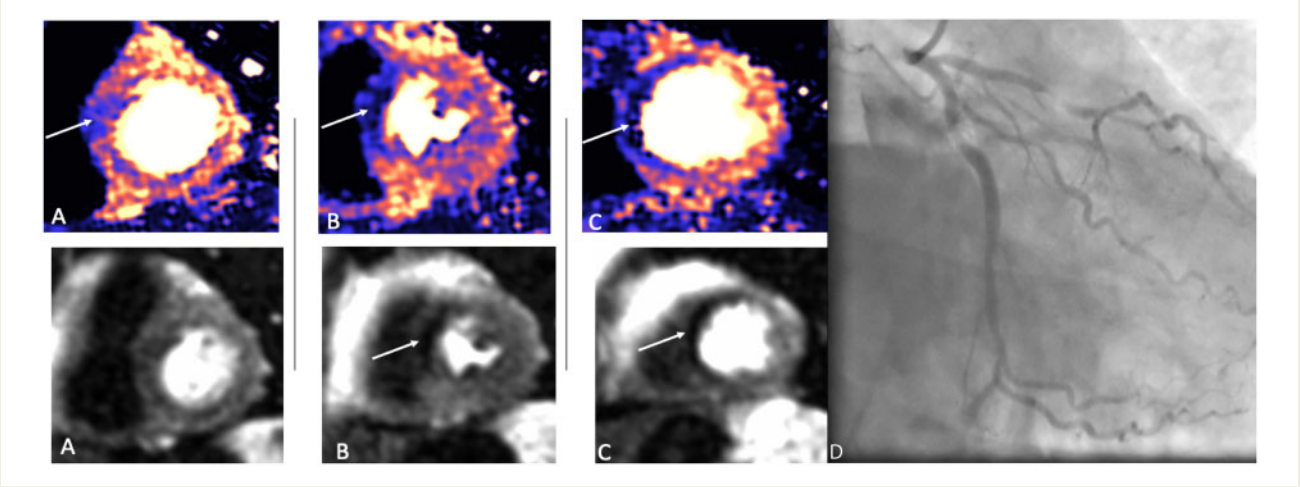

Figure 1 Stress cardiovascular magnetic resonance perfusion study [basal (*A*), mid-cavity (*B*), and apical slices (*C*)] comparing perfusion mapping images (top panel) and traditional gradient echo perfusion images (bottom panel). The perfusion mapping images demonstrate inducible perfusion defect in the septum from base to apex, whilst in the traditional gradient echo perfusion images the inducible perfusion defect in the basal slice is not visible. (*D*) Coronary angiography showing a severe lesion in the mid left anterior descending coronary artery. Courtesy of Professor Marianna Fontana, Royal Free Hospital, London, UK.

preserved LVEF is not infrequent and was independently associated with increased risk of events.

GLS is a strong predictor of adverse cardiovascular outcome in men. However, studies have indicated that GLS may not predict cardiovascular outcomes as effectively in women. Lundorff *et al.*[6] identified echocardiographic predictors of cardiovascular morbidity and mortality in 1245 women from the general population free of HF and atrial fibrillation, who had an echocardiographic examination performed including tissue Doppler imaging. In this subset, 747 women had images eligible for strain analysis. Endpoint was a composite of acute myocardial infarction (MI), HF, and cardiovascular death. During follow-up (median 12.5 years), 162 women (13.0%) reached the composite outcome. These women had higher LV mass index (LVMI), more LV hypertrophy, lower *E*/*A*, higher *E*/*e*′, larger LV dimensions, and longer deceleration time. LVMI and *e*′ remained as significant predictors of the composite outcome. GLS was not an independent predictor of outcome after multivariable adjustment. The authors concluded the degree of LV hypertrophy assessed as LVMI and diastolic dysfunction evaluated by *e*′ were associated with adverse cardiovascular outcome in women from the general population.

Some new technological developments in echocardiography have also been described in some short papers, such as the development of a method of real-time streaming of 3D-transesophageal echocardiography data into head-mounted mixed-reality holographic display allowing for touchless control and data sharing within the cath-lab. The method was tested for the first time in human during percutaneous mitral balloon commissurotomy.[7] In another paper, it was presented a novel fusion pipeline that first aligns 3D echocardiography and magnetic resonance imaging (MRI) in time (mid-diastole) and space using a landmark-based registration algorithm and second fuses both images enabling combined image segmentation for 3D printing. This pipeline was demonstrated in young girl with VSD and straddling mitral valve after an arterial switch operation.[8]

Another outstanding study exploring the use of artificial intelligence in cardiac imaging is that of Ghorbani *et al.*[9] in which a model (Echonet) of deep learning is developed. After training with 2.6 million echocardiograms the model is capable of measuring with good accuracy different cardiac structures and function such as LV end systolic and diastolic volumes (R2 = 0.74 and R2 = 0.70), EF (R2 = 0.50), left atrial enlargement, and LV hypertrophy. Moreover, like other AI models, Echonet is capable to identify phenotypes of age (R2 = 0.46), sex (AUC = 0.88), weight (R2 = 0.56), and height (R2 = 0.33) difficult to assess by human evaluation. Considering that echocardiography is the most widely used imaging test in cardiology, it is anodyne and quite accessible; having the support of AI could reduce the need for human resources in the interpretation of the images allowing the study to be offered to a broader population. Furthermore, it could generate predictive models of cardiovascular events by identifying parameters that are difficult to evaluate by humans.

Finally, in the latest published guidelines, we have appreciated the inclusion of echocardiography with class I recommendation, reflecting the relevance of this technique in routine cardiology practice.[10–13]

Cardiovascular magnetic resonance

Over the last year, cardiovascular magnetic resonance (CMR) has confirmed an established role in the diagnosis, management, and prognosis of patients with chest pain, ischaemic heart disease, and non-ischaemic cardiomyopathies, further improved by AI and machine learning (ML).

The MR-INFORM trial is an unblinded, multicentre, clinical-effectiveness trial in patients with typical angina whose management

was randomly assigned to a CMR stress perfusion-based strategy or an fractional flow reserve (FFR)-based strategy.[14] The primary outcome of death, non-fatal MI, or target-vessel revascularization within 1 year occurred in 15 of 421 patients (3.6%) in the cardiovascular MRI group and 16 of 430 patients (3.7%) in the FFR group [risk difference, -0.2 percentage points; 95% confidence interval (CI) -2.7 to 2.4], demonstrating the non-inferiority of stress CMR to FFR with respect to major adverse cardiac events. Stress CMR was also associated with lower incidence of coronary revascularisation than FFR.

The Stress CMR Perfusion Imaging in the United States (SPINS) study demonstrated excellent diagnostic and prognostic value of stress CMR in single-centre study.[15] Patients with no ischaemia or late gadolinium enhancement (LGE) by CMR ($n = 1583$, 67%) experienced low annualized rates of primary outcome of cardiovascular death or non-fatal MI (<1%) and coronary revascularization (1–3%). In contrast, patients with ischaemia and LGE experienced a more than four-fold higher annual primary outcome rate and a >10-fold higher rate of coronary revascularization during the first year after CMR. The implication is that patients without ischaemia or LGE on CMR have a low incidence of cardiac events, little need for coronary revascularization, and low spending on subsequent ischaemia testing. The cost-effectiveness study of SPINS demonstrated that, stress CMR can be a cost-effective gatekeeping tool prior to invasive coronary angiography (ICA) in patients at risk for obstructive CAD.[16] In particular, the incremental cost-effectiveness ratio for the CMR-based strategy compared with the no-imaging strategy was $52 000/quality-adjusted life years (QALY), whereas the incremental cost-effectiveness ratio for the immediate ICA strategy was $12 million/QALY compared with CMR.

Recent developments on quantitative CMR stress perfusion with automated measurements using AI[17] have been validated clinically.[18] The advances in computation power permit inline automated annotation and the use sophisticated myocardial perfusion models (e.g. the blood-tissue exchange model) to be solved with low variability in real time during scanning vs. hours of complex analysis with potentially variable results (*Figure 1*).

Knott *et al.* assessed the prognostic significance of this new technology in 1 049 patients with known or suspected coronary artery disease reduced myocardial blood flow (MBF) and myocardial perfusion reserve (MPR) quantified automatically inline were strong independent predictors of adverse cardiovascular outcome. For each 1 mL g^{-1} min^{-1} decrease in stress MBF, the adjusted HRs for death and major cardiovascular event (MACE) were 1.93 (95% CI 1.08–3.48; $P = 0.028$) and 2.14 (95% CI 1.58–2.90; $P < 0.0001$), respectively, even after adjusting for age and comorbidities.[19]

AI and ML are providing new opportunities and pushing the envelope in cardiovascular imaging on faster better image analysis. Bhuva *et al.*[20] conducted a multicentre, human and ML CMR study to test generalizability and precision in imaging biomarker analysis. The precision in calculating LVEF in 110 patients with a range a disease, multiple institutions, and different scanner manufacturers and field strengths were similar among expert, trained junior, and automated [coefficient of variation 6.1 (5.2–7.1%), $P = 0.2581$; 8.3 (5.6–10.3%), $P = 0.3653$; 8.8 (6.1–11.1%), $P = 0.8620$]. However, the automated analysis was 186 times faster than humans (0.07 vs. 13 min), concluding that automated ML analysis is faster with similar precision to the most precise (expert) human assessment.

The increasing use of AI in CMR post-processing and image analysis is improving measurements' precision, accuracy and reliability which become less dependent on operator's experience. This can have the direct consequence of empowering less-experienced centres to perform CMR, thus increasing CMR availability. Moreover, the improved diagnostics is also coupled with rapid image analysis which translated in improved physician time of efficiency, an attracting feature for busy clinical schedules.

Up to 30–40% of patients undergoing cardiac resynchronization therapy (CRT) show no improvement, and there is a necessity to improve the selection of patients. In a prospective multicentre study of 200 CRT recipients, Aalen *et al.* demonstrated that the combination of septal and lateral wall function measured by myocardial work with pressure-strain analysis on echocardiography and myocardial scar assessed by CMR LGE can offer a precise and relative simple approach to improve selection of CRT candidates, particularly in patients with ischaemic cardiomyopathy and/or intermediate QRS complex (QRS) duration. CRT response was predicted by the work difference between septum and lateral wall with an area under the curve (AUC) of 0.77 (95% CI 0.70–0.84). The combination of septal viability by CMR combined with myocardial work difference assessment significantly increased predicted CRT response reaching an AUC of 0.88 (95% CI 0.81–0.95).[21]

The role of CMR in the diagnosis of cardiac amyloidosis (CA) is becoming increasingly established. One of the most impactful technical developments this year is the demonstration that a novel approach called diffusion tensor CMR (DT-CMR) can characterize the myocardial microstructural effects of amyloid infiltration in patients. Khalique *et al.* showed that this contrast-free and radiation-free technique can identify the location and extent of the expanded disorganized myocardium. Moreover, novel imaging biomarkers of diffusivity and fractional anisotropy can effectively discriminate CA ($n = 20$) from hypertrophic cardiomyopathy (HCM) ($n = 11$). The preliminary results of this innovative in vivo technique suggest novel pathophysiological mechanisms and improved diagnostics, proving a promising new dimension in the assessment heart muscle disorders.[22]

The Hypertrophic Cardiomyopathy Registry (HCMR Registry) recruited 2755 patients with HCM from 44 sites in 6 countries, and includes CMR, genetic, and biomarkers data in order to improve risk prediction. The baseline data identified two distinct subgroups of patients: a group with sarcomere positive mutation and more fibrosis by CMR and a group sarcomere mutation negative with less fibrosis.[23] The group that was sarcomere mutation positive and more fibrosis had less resting obstruction, whereas the other group had more likely isolated basal septal hypertrophy with obstruction. The degree of obstruction appears an important feature that differs between the two groups.

In a single-centre study, Raman *et al.*[24] investigated the mechanisms of fibrosis progression in patients with HCM. LGE increment was significantly higher in those with impaired MPR < 1.40 and energetics (phosphocreatine/adenosine triphosphate) <1.44 on baseline CMR ($P \leq 0.01$ for both). Substantial LGE progression was associated with LV thinning, LV dilatation, and reduced systolic function and conferred a five-fold increased risk of subsequent clinical events (HR 5.04, 95% CI 1.85–13.79; $P = 0.002$).

Since the beginning of the COVID-19 pandemic, there are an increasing number of publications on the role of CMR in detecting

myocardial damage in infected individuals. Whilst CMR has a clear clinical role in identifying cardiac damage in patients with a range of cardiovascular disease, the results of the CMR studies in COVID-19 patients to date (at the time of writing this manuscript) are still preliminary. Confirmatory results are warranted from large-scale multicentre studies with robust methodology before change in clinical management can be advocated. Most notably, an observational single-centre study in Germany[25] describes the CMR findings in 100 asymptomatic patients recently recovered from the COVID-19 infection (>2 weeks from original diagnosis and resolution of the respiratory symptoms and negative results on a swab test at the end of the isolation period) of whom $n = 67$ recovered at home ($n = 18$ asymptomatic, $n = 49$ minor-to-moderate symptoms) and only $n = 33$ with severe symptoms requiring hospitalization. The cohort was compared to 50 healthy and risk factor-matched controls. They showed that 78 patients (78%) had abnormal CMR findings, including raised myocardial native T1 ($n = 73$), raised myocardial native T2 ($n = 60$), presence of myocardial LGE ($n = 32$), or presence of pericardial enhancement ($n = 22$). At the time of the CMR, high-sensitivity troponin T (hsTnT) was detectable (>3 pg/mL) in 71 patients recently recovered from COVID-19 (71%) and significantly elevated (>13.9 pg/mL) in 5 patients (5%). Compared with healthy controls and risk factor-matched controls, patients recently recovered from COVID-19 had lower LVEF, higher left ventricle volumes, and raised native T1 and T2. Whilst the results of widespread cardiac changes detected by CMR in asymptomatic patients previously infected by the SARS-CoV-2 virus are intriguing, the clinical significance of these findings is unclear and still needs to be determined. Unfortunately, the results of this study have been overemphasized, and in part sensationalized, by the media with the inevitable results of creating concerns among members of the public, confusion among physicians, and a degree of scepticism among imaging experts internationally. Multicentre large-scale prospective CMR studies to detect and measure acute and chronic cardiac damage of the COVID-19 infection are currently underway, COVID-Heart and COVID-PHOSP among others.

The recommendations for the use of CMR in the diagnosis and management of patients with cardiovascular disease are increasing. In the latest release of ESC guidelines in 2020, the Guidelines for the Management of Acute Coronary Syndromes in Patients Presenting without Persistent ST-segment Elevation[12] includes for the first time CMR as a class I recommendation, level of evidence B in all patients with MI and unobstructed coronary arteries without an obvious cause.

Computed tomography

Over the past year, studies concerning computed tomography (CT) in the cardiovascular scenario have strengthened its ability as a predictor of cardiovascular events, and as a therapeutic guide in primary prevention.

Recently, ROBINSCA trial assessed the effectiveness of cardiovascular disease (CVD) screening in asymptomatic participants using the SCORE model ($n = 12\,185$) or coronary artery calcium (CAC) scoring ($n = 12\,950$). Both arms were stratified into low, intermediate, or high 10-year risk for developing fatal and non-fatal cardiovascular disease. SCORE screening arm identified 45.1% at low risk (SCORE <10%), 26.5% at intermediate risk (10–20%), and 28.4% at high risk (≥20%). According to the CAC screening, 76.0% were at low risk (Agatston <100), 15.1% at high risk (100–399), and 8.9% at very high risk (≥400). CAC scoring significantly reduced the proportion of individuals needing preventive treatment compared to SCORE (relative reduction women: 37.2%; men: 28.8%).[26]

From the multicentre CAC Consortium study, 66 636 asymptomatic patients with a CT were assessed, utilizing multivariate regression models for the risk of all-cause mortality and cause-specific mortality based on their CAC score. After adjustments, individuals with CAC ≥1000 had a 5.04-, 6.79-, 1.55-, and 2.89-fold risk of CVD, CAD, cancer, and all-cause mortality, respectively, compared to those with CAC score of 0. The CAC ≥1000 group had a 1.71-, 1.84-, 1.36-, and 1.51-fold increased risk of CVD, CAD, cancer, and all-cause mortality in comparison to those with CAC scores of 400–999. These leads to consider more aggressive preventive treatment for patients with CAC score ≥1000.[27]

The MESA Study investigators assessed the value of CAC for guiding aspirin allocation in primary prevention. All participants ($n = 6470$) underwent a baseline CAC score. CVD risk was estimated using the pooled cohort equation (PCE), defining three strata: <5%, 5–20%, and >20%. Based on PCE the number needed to treat at 5 years (NNT5) was greater than or similar to the number needed to harm (NNH5) among the three estimated cardiovascular risk strata. Conversely, CAC ≥100 and CAC ≥400 identified subgroups in which NNT5 was lower than NNH5. This was true both overall (for CAC ≥100, NNT5 = 140 vs. NNH5 = 518) and within all cardiovascular risk strata. Also, CAC = 0 identified subgroups in which the NNT5 was much higher than the NNH5.[28]

Olesen *et al.* stratified 48 731 patients by diabetes status and CAD severity (no, non-obstructive, or obstructive) assessed by coronary CT angiography (CCTA). With the median follow-up of 3.6 years, they found that diabetic patients had higher death rates than non-diabetic patients, irrespective of CAD severity. Still, those diabetic patients without CAD have a low risk of MI similar to non-diabetic patients.[29]

Finck *et al.* conducted a study with 1615 patients with suspected CAD who underwent a CCTA with morphological analysis of the atheromatous plaque. After an average of 10.5 years, there were 36 cardiac deaths and 15 non-fatal MI. Among characteristics of the plaque; the spotty or gross calcification pattern and the napkin ring sign (NRS) (low-attenuating central portion with ring-like higher attenuation) were predictive for events. Yet, only spotted calcified plaques and NRS convey further prognostic value above clinical features and the severity of coronary stenosis. In a stepwise approach, the prediction of endpoint beyond clinical risk could be improved by including the severity of CAD (x^2 of 27.5, $P < 0.001$) and further discrimination for spotty calcified plaques (x^2 of 3.89, $P = 0.049$).[30]

Another study assessed whether non-calcified low-attenuation plaque burden on CCTA might have a better predictor of MI than CAC or coronary stenosis severity. They followed up 1769 patients with suspected angina for median 4.7 years finding that low-attenuation plaque burden was the strongest predictor of MI ($P = 0.014$), irrespective of cardiovascular risk score, CAC score, or coronary artery stenosis. Patients with low-attenuation plaque burden >4% were almost five times more likely to have subsequent MI ($P < 0.001$).[31]

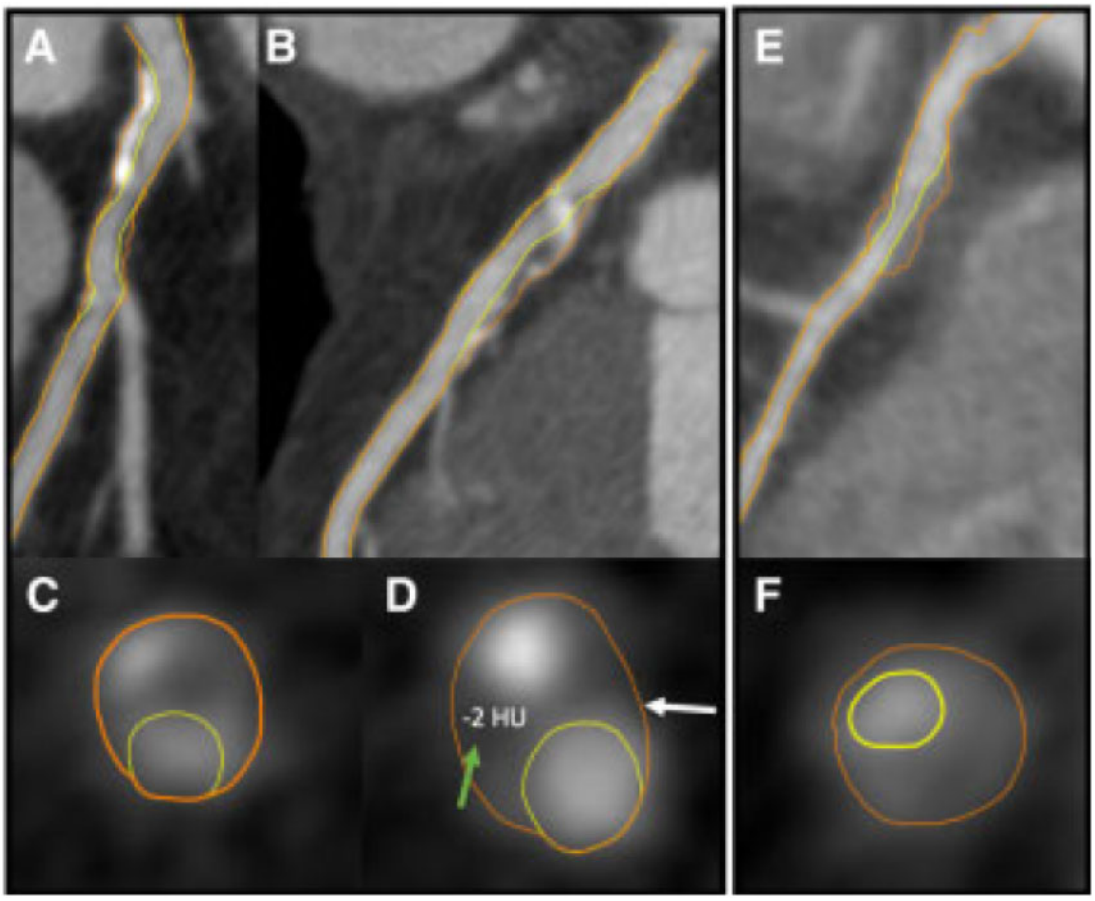

Figure 2 Coronary computed tomography angiograms demonstrating high-risk plaque (HRP) in culprit lesion precursors. A 61-year-old male ex-smoker exhibited a high-risk plaque extending from the (*A*) left main to the (*B*) proximal left anterior descending artery with (*C*) 41% diameter stenosis severity, (*D*) positive remodelling (white arrow), and low-attenuation plaque (green arrow). There is also diffuse calcification. One month later, the patient presented with a non-ST-elevation myocardial infarction. A 55-year-old male with hypertension and hyperlipidaemia exhibited a high-risk plaque with (*E*) only 35% DS severity, but (*F*) positive remodelling, low-attenuation plaque, and napkin-ring sign. The patient presented with a non-ST-elevation myocardial infarction 2 months later. Reproduced with permission from Ferraro *et al.*[33]

From the PARADIGM Study, 2252 patients who underwent clinically indicated serial CCTA at an interscan interval of ≥2 years with non-obstructive plaques (<50%) at baseline were studied. The aim was to prove whether the plaque atheroma volume (PAV), the percentage of diameter stenosis (%DS) or high-risk plaques (HRPs) were more likely to progress to obstructive lesions (>50%). On multivariate analysis, only the baseline total PAV and %DS independently predicted the development of obstructive lesions ($P < 0.05$), whereas the presence of HRP did not ($P > 0.05$).[32]

The investigators of the ICONIC study performed a nested case–control study of patients who underwent a CCTA prior developing an acute coronary syndrome. Culprit lesions were confirmed by invasive coronary angiography and coregistered to baseline CCTA images. They found that HRPs on baseline CCTA were less prevalent in non-obstructive plaques (19.7%) than in obstructive plaques (46.8%). Even though non-obstructive plaque comprised 81.3% of HRP lesions overall. Among patients with identifiable culprit lesion precursors, the adjusted HR was 1.85 (95% CI 1.26–2.72) for HRP, with no interaction between %DS and HRP. Compared to non-obstructive HRP lesions, obstructive lesions without HRP exhibited a non-significant HR of 1.41 (95% CI 0.61–3.25) (*Figure 2*).[33]

Recently, the ADVANCE Registry presented its 1-year results of 4288 patients with suspected CAD in whom a 30% coronary stenosis was identified by CCTA. They evaluated the relationship of fractional flow reserve derived from CCTA (FFR_{CT}) with clinical outcomes. There were 55 events; 78% of them occurred in patients with an FFR_{CT} ≤0.80 ($P = 0.06$). Time to first event (cardiovascular death or MI) occurred more in patients with an FFR_{CT} ≤0.80 compared with FFR_{CT} >0.80 patients (25 [0.80%] vs. 3 [0.20%]; relative risk (RR): 4.22; 95% CI: 1.28–13.95; $P = 0.01$). Concerning the downstream care, the majority of patients in whom medical therapy was the recommended treatment strategy following FFR_{CT} continued on only medical therapy at 1 year (92.9%), and when the site recommendation was for revascularization, the majority (68.9%) were revascularized.[34]

An innovative study introduces a new parameter of dynamic CT perfusion (CTP) called stress MBF rate (SFR). This is defined as the

ratio of hyperaemic (ATP infusion) MBF in an artery with stenosis to the hyperaemic MBF in a non-diseased artery. Eighty-two patients were derived to invasive angiography for suspected CAD. Stress dynamic CTP and CCTA was performed before invasive angiography. Out of 101 vessels with 30–90% stenosis on invasive angiography, FFR resulted hemodynamically significant (<0.80) in 47.5% of them. SFR was lower for invasive FFR < 0.80 lesions (0.66 vs. 0.90; $P < 0.01$). Compared with ≥50% stenosis by computed tomography angiography (CTA), the specificity for detecting ischaemia by SFR increased from 43% to 91%, whilst the sensitivity decreased from 95% to 62%. The combination of stenosis ≥50% by CTA and SFR resulted in an AUC of 0.91, which was significantly higher than MBF alone.[35]

Nuclear imaging

Nowadays, the potential survival benefit of ischaemia-guided early coronary revascularization in patients with stable coronary artery disease (CAD) is still in debate.

Patel *et al.* performed a single-centre cohort study including 16 029 patients with suspected or known CAD (mean age 68.6 ± 11.9 years) who underwent a Rubidium-82 (Rb82) rest-stress positron emission tomography (PET) myocardial perfusion imaging (MPI), excluding those with LVEF < 40%. After a median follow-up of 3.7 years, 1277 patients underwent early revascularization (87% PCI, 13% CABG), and 2493 (15.6%) died. After a propensity score adjustment for potential confounders, a Cox model found an interaction between %ischaemia and early revascularization ($P < 0.001$ for both all-cause and cardiac death). They also report medical therapy survival equipoise at 5% ischaemia. This ischaemia threshold for survival benefit is lower than previously reported with single photon emission CT (SPECT) MPI.[36]

In a phase-III prospective multicentric clinical study, the novel PET MPI tracer Fluorine-18 flurpiridaz is evaluated for its diagnostic efficacy detecting significant CAD (>50% stenosis in quantitative ICA) vs. SPECT. 755 patients (mean age 62.3 ± 9.5 years) were included. The PET MPI with the novel tracer demonstrated to have superior sensitivity than SPECT [71.9%, 95% CI 67.0–76.3%; $P < 0.001$ vs. 53.7% (95% CI: 48.5–58.8%)]. It was also superior to SPECT for defect size ($P < 0.001$), image quality ($P < 0.001$), diagnostic certainty ($P < 0.001$), and radiation exposure (6.1 ± 0.4 vs. 13.4 ± 3.2 mSv; $P < 0.001$). This is a new diagnostic tool with better diagnostic performance comparing to SPECT, in particular for women, obese, and patients undergoing pharmacological stress testing.[37,38]

Kwiecinski *et al.* presented a *post hoc* analysis of 293 patients with previous CAD who underwent 18-F-NaF PET. Of those, 203 (69%) showed increased coronary activity [represented by quantitative coronary microcalcification activity (CME)]. After a median follow-up of 42 months, 20 patients (7%) experienced fatal or non-fatal MI. All of them presented previously increased coronary 18F-NaF activity. On an ROC analysis, MI prediction was better for 18F-NaF CME score than coronary calcium scoring and different clinical risk scores. This represents a powerful and safe tool for the detection of coronary atherosclerotic inflammation.[39]

Another proof of improvements of imaging's ability to predict events is the international multicentre study by Miller *et al.* in which they sought to determine the interactions between SPECT-MPI ischaemia, high-risk non-perfusion SPECT-MPI findings and MACE. In total, 16 578 patients with known or suspected CAD were analysed. Transient ischaemic dilation (TID) and post-stress wall motion abnormalities (WMA) were non-perfusion markers of ischaemia. After a median follow-up of 4.7 years, 1842 individuals presented one event. In a univariate analysis, the authors found that patients with mild ischaemia (<10%) and TID were more likely to present MACE compared with patients without TID (adjusted HR 1.42, $P = 0.023$). There were similar findings in patients with post-stress WMA. However, multivariable analysis of patients with mild ischaemia, TID (adjusted HR 1.50, $P = 0.037$), but not WMA, was independently associated with increased MACE.[40]

Heart to mediastinum (H/M) ratio measured by cardiac 123I-metaiodobenzylguanidine (123I-mIBG) scintigraphy has demonstrated prognostic significance in the setting of chronic HF. The OPAR Registry investigators describe a single-centre observational cohort study with 349 patients admitted for acute decompensated HF. 123I-MIBG imaging and echocardiography were performed before discharge. Of those 127 presented reduced EF, 78 mid-range EF, and 144 preserved EF. After a median follow-up period of 2.1 (±1.4) years, 128 patients presented cardiac events (HF hospitalization or cardiac death). A multivariable Cox analysis demonstrates that late H/M (after 200 min of tracer) was significantly associated with cardiac events in overall cohort ($P = 0.0038$), as in each EF subgroup ($P = 0.0235$ in reduced, $P = 0.0119$ in mid-range and $P = 0.0311$ in preserved). The authors conclude that H/M ratio reflects cardiac sympathetic nerve dysfunction, which is associated with cardiac events in acute HF patients, irrespective of EF.[41]

One-third of chronic HF patients who assign to CRT therapy based on guidelines classical eligibility criteria does not present benefits. Verschure *et al.* presented their results in 78 stable HF individuals with guideline-based criteria for CRT who underwent a cardiac 123I-mIBG imaging before device implantation. Late H/M ratio was an independent predictor of LVEF improvement to >35% ($P = 0.0014$) and early H/M for LVEF improvement of at least 10% from basal.[42]

CA implies ominous prognosis for patients. Early diagnosis with sufficient accuracy and safety remain still challenging. Rosengren *et al.* published the largest study of CA patients (both AL and ATTR) examined with Pittsburgh compound (11C-PIB) PET. In this study, the diagnostic accuracy of 11C-PIB PET is remarkable with high sensitivity (94%) and specificity (93% to 100%) for distinguishing CA patients from both non-amyloid hypertrophic and healthy controls. 11C-PIB uptake was significantly higher in AL-CA patients than in ATTR-CA patients ($P < 0.001$). In the study from Lee *et al.*, they also demonstrate correlation between 11C-PIB uptake and myocardial histology in CA. In addition, after a median follow-up of 423 days, the degree of myocardial 11C-PIB uptake was a significant predictor of clinical outcome (death, heart transplantation, and acute decompensated HF) on multivariate Cox regression analysis (adjusted HR: 1.185; 95% CI 1.054–1.332; $P = 0.005$).[43]

Roque *et al.* used serial 18F-fluorodeoxyglucose (FDG PET/CT) after 1, 6, and 12 months in 37 post-aortic or mitral valve replacement patients. They obtained the standardized uptake values (SUVs) and a new proposed value denominate valve uptake index [(SUVmax - SUVmean)/SUVmax]. Of the 111 PET/CT performed, FDG uptake was visually detectable in 79.3% of patients, presenting a diffuse, homogeneous distribution pattern in 93%. No patient

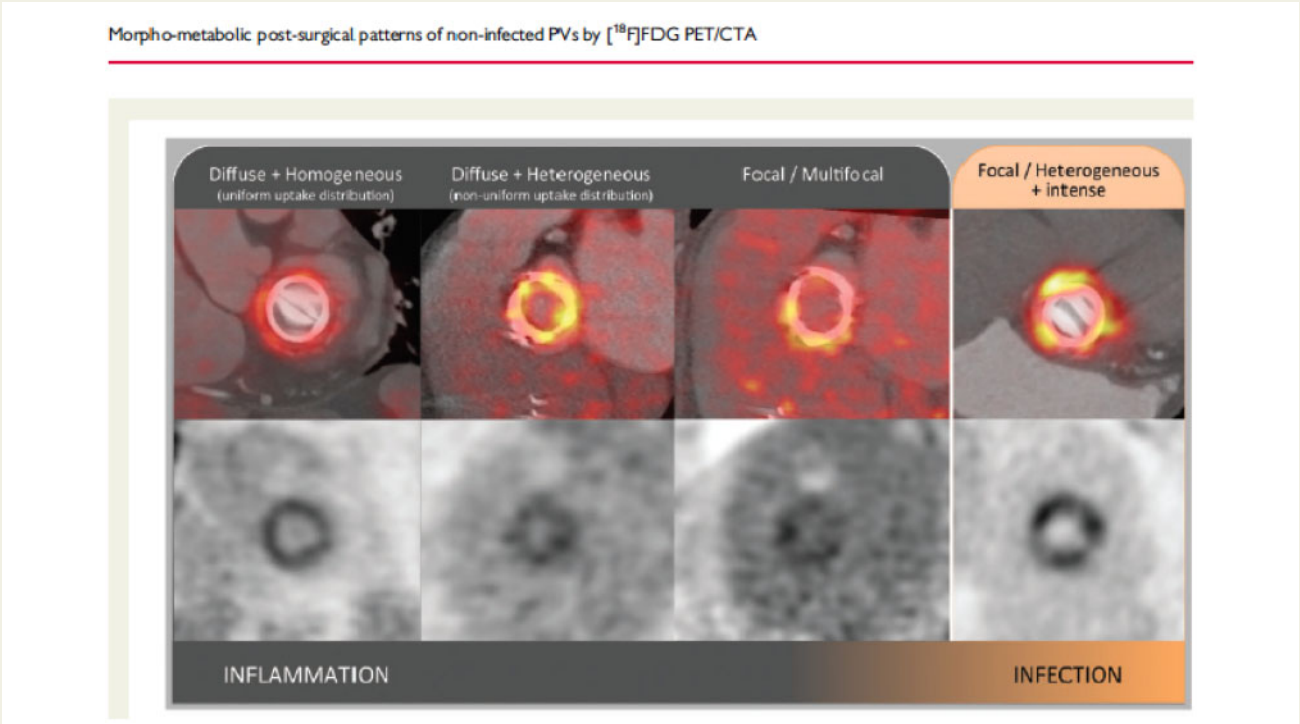

Figure 3 18F-fluorodeoxyglucose uptake distribution patterns (visual assessment). 18F-fluorodeoxyglucose uptake in non-infected prostheses (left panel), compared with an example of prosthetic valve endocarditis (right panel). Positron emission tomography/CTA fusion images of the valve plane (upper row), and their corresponding attenuation-corrected positron emission tomography images (lower row). From left to right, the characteristic inflammation patterns in order of descending frequency: diffuse homogeneous (93%), diffuse heterogeneous (7%), and focal/multifocal (2%). The diffuse homogeneous pattern is characteristic of inflammation and clearly differentiable from infection, whereas more focal. 18F-fluorodeoxyglucose uptake may overlap with infective endocarditis. No anatomic lesions were detected in any patient. Reproduced with permission from Roque *et al.*[44]

presented endocarditis during follow-up (*Figure 3*). Surprisingly, no significant differences were encountered in FDG distribution or uptake values between 1, 6, or 12 months, questioning the 3-month post-surgical period for the assessment of prosthetic infection.[44]

Tam *et al.* presented a study of FDG PET/CT in suspected LV assist devices (LVAD) associating their single-centre retrospective cases between September 2015 and February 2018 with a systematic review of PubMed from database inception through March 2018 involving in total 119 scans. Pooled sensitivity was 92% (95% CI: 82%–97%) and specificity was 83% (95% CI: 24%–99%) for FDG PET/CT in diagnosing LVAD infections. The ROC curve analysis demonstrated an AUC of 0.94 (95% CI 0.91–0.95).[45]

Another infectious scenario in which nuclear imaging techniques play an important diagnostic role is cardiac device-related infected endocarditis (CDRIE). Holcman *et al.* assessed the diagnostic accuracy of the hybrid technique of SPECT CT with technetium99mhexamethylpropyleneamine oxime-labelled leucocytes (99mTc-HMPAO-SPECT/CT). In a single-centre prospective study, 103 patients with suspected CDRIE who underwent 99mTc-HMPAO-SPECT/CT were included. They found that adding this nuclear technique improves the sensitivity of the modified Duke criteria alone (87% vs. 48%, $P < 0.001$), whereas a negative scan excludes CDRIE with high probability. This yielded a reduction in possible CDRIE diagnoses.[46]

Data availability

The data underlying this article will be shared on reasonable request to the corresponding author.

Conflict of interest: none declared.

References

1. Maron DJ, Hochman JS, Reynolds HR, Bangalore S, O'Brien SM, Boden WE, Chaitman BR, Senior R, López-Sendón J, Alexander KP, Lopes RD, Shaw LJ, Berger JS, Newman JD, Sidhu MS, Goodman SG, Ruzyllo W, Gosselin G, Maggioni AP, White HD, Bhargava B, Min JK, Mancini GBJ, Berman DS, Picard MH, Kwong RY, Ali ZA, Mark DB, Spertus JA, Krishnan MN, Elghamaz A, Moorthy N, Hueb WA, Demkow M, Mavromatis K, Bockeria O, Peteiro J, Miller TD, Szwed H, Doerr R, Keltai M, Selvanayagam JB, Steg PG, Held C, Kohsaka S, Mavromichalis S, Kirby R, Jeffries NO, Harrell FE, Rockhold FW, Broderick S, Ferguson TB, Williams DO, Harrington RA, Stone GW, Rosenberg Y; ISCHEMIA Research Group. Initial invasive or conservative strategy for stable coronary disease. *N Engl J Med* 2020;**382**:1395–1407.
2. Budoff MJ, Mayrhofer T, Ferencik M, Bittner D, Lee KL, Lu MT, Coles A, Jang J, Krishnam M, Douglas PS, Hoffmann U; PROMISE Investigators. Prognostic value of coronary artery calcium in the PROMISE study (Prospective Multicenter Imaging Study for Evaluation of Chest Pain). *Circulation* 2017;**136**:1993–2005.
3. Chacko L, Martone R, Bandera F, Lane T, Martinez-Naharro A, Boldrini M, Rezk T, Whelan C, Quarta C, Rowczenio D, Gilbertson JA, Wongwarawipat T, Lachmann H, Wechalekar A, Sachchithanantham S, Mahmood S, Marcucci R, Knight D, Hutt D, Moon J, Petrie A, Cappelli F, Guazzi M, Hawkins PN, Gillmore JD, Fontana M. Echocardiographic phenotype and prognosis in transthyretin cardiac amyloidosis. *Eur Heart J* 2020;**41**:1439–1447.

4. Tsugu T, Postolache A, Dulgheru R, Sugimoto T, Tridetti J, Nguyen Trung ML, Piette C, Moonen M, Manganaro R, Ilardi F, Chitroceanu AM, Sperlongano S, Go YY, Kacharava G, Athanassopoulos GD, Barone D, Baroni M, Cardim N, Hagendorff A, Hristova K, Lopez T, de la Morena G, Popescu BA, Penicka M, Ozyigit T, Rodrigo Carbonero JD, van de Veire N, Von Bardeleben RS, Vinereanu D, Zamorano JL, Rosca M, Calin A, Magne J, Cosyns B, Galli E, Donal E, Santoro C, Galderisi M, Badano LP, Lang RM, Lancellotti P. Echocardiographic reference ranges for normal left ventricular layer-specific strain: results from the EACVI NORRE study. *Eur Heart J Cardiovasc Imaging* 2020;**21**:896–905.
5. Kong WKF, Vollema EM, Prevedello F, Perry R, Ng ACT, Poh KK, Almeida AG, González A, Shen M, Yeo TC, Shanks M, Popescu BA, Galian Gay L, Fijałkowski M, Liang M, Chen RW, Ajmone Marsan N, Selvanayagam J, Pinto F, Zamorano JL, Pibarot P, Evangelista A, Delgado V, Bax JJ. Prognostic implications of left ventricular global longitudinal strain in patients with bicuspid aortic valve disease and preserved left ventricular ejection fraction. *Eur Heart J Cardiovasc Imaging* 2020;**21**:759–767.
6. Lundorff I, Modin D, Mogelvang R, Godsk Jørgensen P, Schnohr P, Gislason G, Biering-Sørensen T. Echocardiographic predictors of cardiovascular morbidity and mortality in women from the general population. *Eur Heart J Cardiovasc Imaging* 2020;doi:10.1093/ehjci/jeaa167.
7. Kasprzak JD, Pawlowski J, Peruga JZ, Kaminski J, Lipiec P. First-in-man experience with real-time holographic mixed reality display of three-dimensional echocardiography during structural intervention: balloon mitral commissurotomy. *Eur Heart J* 2019;**41**:801.
8. Gomez A, Gomez G, Simpson J, Valverde I. 3D hybrid printed models in complex congenital heart disease: 3D echocardiography and cardiovascular magnetic resonance imaging fusion. *Eur Heart J* 2020;**41**:ehaa654–4214.
9. Ghorbani A, Ouyang D, Abid A, He B, Chen JH, Harrington RA, Liang DH, Ashley EA, Zou JY. Deep learning interpretation of echocardiograms. *NPJ Digit Med* 2020;**3**:10.
10. Hindricks G, Potpara T, Dagres N, Arbelo E, Bax JJ, Blomström-Lundqvist C, Boriani G, Castella M, Dan GA, Dilaveris PE, Fauchier L, Filippatos G, Kalman JM, La Meir M, Lane DA, Lebeau JP, Lettino M, Lip GYH, Pinto FJ, Thomas GN, Valgimigli M, Van Gelder IC, Van Putte BP, Watkins CL; ESC Scientific Document Group. 2020 ESC Guidelines for the diagnosis and management of atrial fibrillation developed in collaboration with the European Association of Cardio-Thoracic Surgery (EACTS). *Eur Heart J* 2020.10.1093/eurheartj/ehaa612.
11. Baumgartner H, De Backer J, Babu-Narayan SV, Budts W, Chessa M, Diller GP, Lung B, Kluin J, Lang IM, Meijboom F, Moons P, Mulder BJM, Oechslin E, Roos-Hesselink JW, Schwerzmann M, Sondergaard L, Zeppenfeld K; ESC Scientific Document Group. 2020 ESC Guidelines for the management of adult congenital heart disease. *Eur Heart J* 2020. 10.1093/eurheartj/ehaa554.
12. Collet JP, Thiele H, Barbato E, Barthélémy O, Bauersachs J, Bhatt DL, Dendale P, Dorobantu M, Edvardsen T, Folliguet T, Gale CP, Gilard M, Jobs A, Jüni P, Lambrinou E, Lewis BS, Mehilli J, Meliga E, Merkely B, Mueller C, Roffi M, Rutten FH, Sibbing D, Siontis GCM; ESC Scientific Document Group. 2020 ESC Guidelines for the management of acute coronary syndromes in patients presenting without persistent ST-segment elevation. *Eur Heart J* 2020. 10.1093/eurheartj/ehaa575.
13. Pelliccia A, Sharma S, Gati S, Bäck M, Börjesson M, Caselli S, Collet JP, Corrado D, Drezner JA, Halle M, Hansen D, Heidbuchel H, Myers J, Niebauer J, Papadakis M, Piepoli MF, Prescott E, Roos-Hesselink JW, Graham Stuart A, Taylor RS, Thompson PD, Tiberi M, Vanhees L, Wilhelm M; ESC Scientific Document Group. 2020 ESC Guidelines on sports cardiology and exercise in patients with cardiovascular disease. *Eur Heart J* 2020.10.1093/eurheartj/ehaa605.
14. Nagel E, Greenwood JP, McCann GP, Bettencourt N, Shah AM, Hussain ST, Perera D, Plein S, Bucciarelli-Ducci C, Paul M, Westwood MA, Marber M, Richter WS, Puntmann VO, Schwenke C, Schulz-Menger J, Das R, Wong J, Hausenloy DJ, Steen H, Berry C; MR-INFORM Investigators. Magnetic resonance perfusión or fraction flow reserve in coronary disease. *N Engl J Med* 2019;**380**:2418–2428.
15. Kwong RY, Ge Y, Steel K, Bingham S, Abdullah S, Fujikura K, Wang W, Pandya A, Chen YY, Mikolich JR, Boland S, Arai AE, Bandettini WP, Shanbhag SM, Patel AR, Narang A, Farzaneh-Far A, Romer B, Heitner JF, Ho JY, Singh J, Shenoy C, Hughes A, Leung SW, Marji M, Gonzalez JA, Mehta S, Shah DJ, Debs D, Raman SV, Guha A, Ferrari VA, Schulz-Menger J, Hachamovitch R, Stuber M, Simonetti OP. Cardiac magnetic resonance stress perfusion imaging for evaluation of patients with chest pain. *J Am Coll Cardiol* 2019;**74**:1741–1755.
16. Ge Y, Pandya A, Steel K, Bingham S, Jerosch-Herold M, Chen YY, Mikolich JR, Arai AE, Bandettini WP, Patel AR, Farzaneh-Far A, Heitner JF, Shenoy C, Leung SW, Gonzalez JA, Shah DJ, Raman SV, Ferrari VA, Schulz-Menger J, Hachamovitch R, Stuber M, Simonetti OP, Kwong RY. Cost effectiveness analysis of stress cardiovascular magnetic resonance Imaging for stable chest pain syndromes. *JACC Cardiovasc Imaging* 2020;**13**:1505–1517.
17. Kellman P, Hansen MS, Nielles-Vallespin S, Nickander J, Themudo R, Ugander M, Xue H. Myocardial perfusion cardiovascular magnetic resonance: optimized dual sequence and reconstruction for quantification. *J Cardiovasc Magn Reson* 2017;**19**:43.
18. Kotecha T, Martinez-Naharro A, Boldrini M, Knight D, Hawkins P, Kalra S, Patel D, Coghlan G, Moon J, Plein S, Lockie T, Rakhit R, Patel N, Xue H, Kellman P, Fontana M. Automated pixel-wise quantitative myocardial perfusion mapping by CMR to detect obstructive coronary artery disease and coronary microvascular dysfunction: validation against invasive coronary physiology. *JACC Cardiovasc Imaging* 2019;**12**:1958–1969.
19. Knott KD, Seraphim A, Augusto JB, Xue H, Chacko L, Aung N, Petersen SE, Cooper JA, Manisty C, Bhuva AN, Kotecha T, Bourantas CV, Davies RH, Brown LAE, Plein S, Fontana M, Kellman P, Moon JC. The prognostic significance of quantitative myocardial perfusion: an artificial intelligence-based approach using perfusion mapping. *Circulation* 2020;**141**:1282–1291.
20. Bhuva AN, Bai W, Lau C, Davies RH, Ye Y, Bulluck H, McAlindon E, Culotta V, Swoboda PP, Captur G, Treibel TA, Augusto JB, Knott KD, Seraphim A, Cole GD, Petersen SE, Edwards NC, Greenwood JP, Bucciarelli-Ducci C, Hughes AD, Rueckert D, Moon JC, Manisty CH. A multicentre, scan-rescan, human and machine learning CMR Study to test generalizability and precision in Imaging biomaker analisis. *Circ Cardiovasc Imaging* 2019;**12**:e009214.
21. Aalen JM, Donal E, Larsen CK, Duchenne J, Lederlin M, Cvijic M, Hubert A, Voros G, Leclercq C, Bogaert J, Hopp E, Fjeld JG, Penicka M, Linde C, Aalen OO, Kongsgård E, Galli E, Voigt JU, Smiseth OA. Imaging predictors of response to cardiac resynchronization therapy: left ventricular work asymmetry by echocardiography and septal viability by cardiac magnetic resonance. *Eur Heart J* 2020;**41**:3813–3823.
22. Khalique Z, Ferreira PF, Scott AD, Nielles-Vallespin S, Martinez-Naharro A, Fontana M, Hawkins P, Firmin DN, Pennell DJ. Diffusion tensor cardiovascular magnetic resonance in cardiac amyloidosis. *Circ Cardiovasc Imaging* 2020;**13**:e009901.
23. Neubauer S, Kolm P, Ho CY, Kwong RY, Desai MY, Dolman SF, Appelbaum E, Desvigne-Nickens P, DiMarco JP, Friedrich MG, Geller N, Harper AR, Jarolim P, Jerosch-Herold M, Kim D-Y, Maron MS, Schulz-Menger J, Piechnik SK, Thomson K, Zhang C, Watkins H, Weintraub WS, Kramer CM, Mahmod M, Jacoby D, White J, Chiribiri A, Helms A, Choudhury L, Michels M, Bradlow W, Salerno M, Heitner S, Prasad S, Mohiddin S, Swoboda P, Mahrholdt H, Bucciarelli-Ducci C, Weinsaft J, Kim H, McCann G, van Rossum A, Williamson E, Flett A, Dawson D, Mongeon FP, Olivotto I, Crean A, Owens A, Anderson L, Biagini E, Newby D, Berry C, Kim B, Larose E, Abraham T, Sherrid M, Nagueh S, Rimoldi O, Elstein E, Autore C, Kramer CM; HCMR Investigators. Distinct subgroups in hypertrophic cardiomyopathy from the NHLBI HCM Registry. *J Am Coll Cardiol* 2019;**74**:2333–2345.
24. Raman B, Ariga R, Spartera M, Sivalokanathan S, Chan K, Dass S, Petersen SE, Daniels MJ, Francis J, Smillie R, Lewandowski AJ, Ohuma EO, Rodgers C, Kramer CM, Mahmod M, Watkins H, Neubauer S. Progression of myocardial fibrosis in hypertrophic cardiomyopathy: mechanisms and clinical implications. *Eur Heart J Cardiovasc Imaging* 2019;**20**:157–167.
25. Puntmann VO, Carerj ML, Wieters I, Fahim M, Arendt C, Hoffmann J, Shchendrygina A, Escher F, Vasa-Nicotera M, Zeiher AM, Vehreschild M, Nagel E. Outcomes of cardiovascular magnetic resonance imaging in patients recently recovered from coronavirus disease 2019 (COVID-19). *JAMA Cardiol* 2020;**5**:e203557.
26. Aalst C V D, Denissen SJAM, Vonder M, Gratama JWC, Adriaansen HJ, Kuijpers D, Vliegenthart R, Lennep J. V, P van der H, Braam RL, Prm van Dijkman, van Bruggen R, Oudkerk H. D., Koning H. D. Screening for cardiovascular disease risk using traditional risk factor assessment or coronary artery calcium scoring: the ROBINSCA trial. *Eur Heart J Cardiovasc Imaging* 2020;**21**(11):1216–1224.
27. Peng AW, Mirbolouk M, Orimoloye OA, Osei AD, Dardari Z, Dzaye O, Budoff MJ, Shaw L, Miedema MD, Rumberger J, Berman DS, Rozanski A, Al-Mallah MH, Nasir K, Blaha MJ. Long-term all-cause and cause-specific mortality in asymptomatic patients with CAC ≥1,000. *JACC Cardiovasc Imaging* 2020;**13**:83–93.
28. Cainzos-Achirica M, Miedema MD, McEvoy JW, Al Rifai M, Greenland P, Dardari Z, Budoff M, Blumenthal RS, Yeboah J, Duprez DA, Mortensen MB, Dzaye O, Hong J, Nasir K, Blaha MJ. Coronary artery calcium for personalized allocation of aspirin in primary prevention of cardiovascular disease in 2019: the MESA Study (Multi-Ethnic Study of Atherosclerosis). *Circulation* 2020;**141**:1541–1553.
29. Olesen KKW, Riis AH, Nielsen LH, Steffensen FH, Nørgaard BL, Jensen JM, Poulsen PL, Thim T, Bøtker HE, Sørensen HT, Maeng M. Risk stratification by assessment of coronary artery disease using coronary computed tomography angiography in diabetes and non-diabetes patients: a study from the Western Denmark Cardiac Computed Tomography Registry. *Eur Heart J Cardiovasc Imaging* 2019;**20**:1271–1278.
30. Finck T, Stojanovic A, Will A, Hendrich E, Martinoff S, Hausleiter J, Hadamitzky M. Long-term prognostic value of morphological plaque features on coronary

computed tomography angiography. *Eur Heart J Cardiovasc Imaging* 2020;**21**(3):237–248.
31. Williams MC, Kwiecinski J, Doris M, McElhinney P, D'Souza MS, Cadet S, Adamson PD, Moss AJ, Alam S, Hunter A, Shah ASV, Mills NL, Pawade T, Wang C, Weir McCall J, Bonnici-Mallia M, Murrills C, Roditi G, Beek E. V, Shaw LJ, Nicol ED, Berman DS, Slomka PJ, Newby DE, Dweck MR, Dey D. Low-attenuation noncalcified plaque on coronary computed tomography angiography predicts myocardial infarction: results from the multicenter SCOT-HEART Trial (Scottish Computed Tomography of the HEART). *Circulation* 2020;**141**: 1452–1462.
32. Lee S-E, Sung JM, Andreini D, Budoff MJ, Cademartiri F, Chinnaiyan K, Choi JH, Chun EJ, Conte E, Gottlieb I, Hadamitzky M, Kim YJ, Kumar A, Lee BK, Leipsic JA, Maffei E, Marques H, Pontone G, Raff G, Shin S, Stone PH, Samady H, Virmani R, Narula J, Berman DS, Shaw LJ, Bax JJ, Lin FY, Min JK, Chang H-J. Differential association between the progression of coronary artery calcium score and coronary plaque volume progression according to statins: the Progression of AtheRosclerotic PlAque DetermIned by Computed TomoGraphic Angiography Imaging (PARADIGM) study. *Eur Heart J Cardiovasc Imaging* 2019;**20**:1307–1314.
33. Ferraro RA, Rosendael A. V, Lu Y, Andreini D, Al-Mallah MH, Cademartiri F, Chinnaiyan K, Chow BJW, Conte E, Cury RC, Feuchtner G, Araújo Gonçalves P. D, Hadamitzky M, Kim Y-J, Leipsic J, Maffei E, Marques H, Plank F, Pontone G, Raff GL, Villines TC, Lee S-E, Al'Aref SJ, Baskaran L, Cho I, Danad I, Gransar H, Budoff MJ, Samady H, Stone PH. Non-obstructive high-risk plaques increase the risk of future culprit lesions comparable to obstructive plaques without high-risk features: the ICONIC study. *Eur Heart J Cardiovasc Imaging* 2020;**21**(9):973–980.
34. Patel MR, Nørgaard BL, Fairbairn TA, Nieman K, Akasaka T, Berman DS, Raff GL, Hurwitz Koweek LM, Pontone G, Kawasaki T, Sand NPR, Jensen JM, Amano T, Poon M, Øvrehus KA, Sonck J, Rabbat MG, Mullen S, De Bruyne B, Rogers C, Matsuo H, Bax JJ, Leipsic J. 1-Year impact on medical practice and clinical outcomes of FFRCT. *JACC Cardiovasc Imaging* 2020;**13**:97–105.
35. Yang J, Dou G, He B, Jin Q, Chen Z, Jing J, Di Carli MF, Chen Y, Blankstein R. Stress myocardial blood flow ratio by dynamic CT perfusion identifies hemodynamically significant CAD. *JACC Cardiovasc Imaging* 2020;**13**:966–976.
36. Patel KK, Spertus JA, Chan PS, Sperry BW, Thompson RC, Al Badarin F, Kennedy KF, Case JA, Courter S, Saeed IM, McGhie AI, Bateman TM. Extent of myocardial ischemia on positron emission tomography and survival benefit with early revascularization. *J Am Coll Cardiol* 2019;**74**:1645–1654.
37. Maddahi J, Lazewatsky J, Udelson JE, Berman DS, Beanlands RSB, Heller GV, Bateman TM, Knuuti J, Orlandi C. Phase-III clinical trial of fluorine-18 flurpiridaz positron emission tomography for evaluation of coronary artery disease. *J Am Coll Cardiol* 2020;**76**:391–401.
38. Joshi NV, Vesey AT, Williams MC, Shah ASV, Calvert PA, Craighead FHM, Yeoh SE, Wallace W, Salter D, Fletcher AM, van Beek EJR, Flapan AD, Uren NG, Behan MWH, Cruden NLM, Mills NL, Fox KAA, Rudd JHF, Dweck MR, Newby DE. 18F-fluoride positron emission tomography for identification of ruptured and high-risk coronary atherosclerotic plaques: a prospective clinical trial. *Lancet* 2014;**383**:705–713.
39. Kwiecinski J, Tzolos E, Adamson PD, Cadet S, Moss AJ, Joshi N, Williams MC, van Beek EJR, Dey D, Berman DS, Newby DE, Slomka PJ, Dweck MR. Coronary 18F-sodium fluoride uptake predicts outcomes in patients with coronary artery disease. *J Am Coll Cardiol* 2020;**75**:3061–3074.
40. Miller RJH, Hu L-H, Gransar H, Betancur J, Eisenberg E, Otaki Y, Sharir T, Fish MB, Ruddy TD, Dorbala S, Carli MD, Einstein AJ, Kaufmann PA, Sinusas AJ, Miller EJ, Bateman T, Germano G, Tamarappoo BK, Dey D, Berman DS, Slomka PJ. Transient ischaemic dilation and post-stress wall motion abnormality increase risk in patients with less than moderate ischaemia: analysis of the REFINE SPECT registry. *Eur Heart J Cardiovasc Imaging* 2020;**21**:567–575.
41. Seo M, Yamada T, Tamaki S, Watanabe T, Morita T, Furukawa Y, Kawasaki M, Kikuchi A, Kawai T, Abe M, Nakamura J, Yamamoto K, Kayama K, Kawahira M, Tanabe K, Kimura T, Ueda K, Sakamoto D, Sakata Y, Fukunami M. Prognostic significance of cardiac I-123-metaiodobenzylguanidine imaging in patients with reduced, mid-range, and preserved left ventricular ejection fraction admitted for acute decompensated heart failure: a prospective study in Osaka Prefectural Acute Heart Failure Registry (OPAR). *Eur Heart J Cardiovasc Imaging* 2020;doi: 10.1093/ehjci/jeaa025.
42. Verschure DO, Poel E, De Vincentis G, Frantellizzi V, Nakajima K, Gheysens O, Groot J. D, Verberne HJ. The relation between cardiac 123I-mIBG scintigraphy and functional response 1 year after CRT implantation. *Eur Heart J Cardiovasc Imaging* 2020;doi: 10.1093/ehjci/jeaa045.
43. Rosengren S, Skibsted Clemmensen T, Tolbod L, Granstam S-O, Eiskjær H, Wikström G, Vedin O, Kero T, Lubberink M, Harms HJ, Flachskampf FA, Baron T, Carlson K, Mikkelsen F, Antoni G, Frost Andersen N, Hvitfeldt Poulsen S, Sörensen J. Diagnostic accuracy of [11C]PIB positron emission tomography for detection of cardiac amyloidosis. *JACC Cardiovasc Imaging* 2020;**13**:1337–1347.
44. Roque A, Pizzi MN, Fernández-Hidalgo N, Permanyer E, Cuellar-Calabria H, Romero-Farina G, Ríos R, Almirante B, Castell-Conesa J, Escobar M, Ferreira-González I, Tornos P, Aguadé-Bruix S. Morpho-metabolic post-surgical patterns of non-infected prosthetic heart valves by [18F]FDG PET/CTA: "normality" is a possible diagnosis. *Eur Heart J Cardiovasc Imaging* 2020;**21**:24–33.
45. Tam MC, Patel VN, Weinberg RL, Hulten EA, Aaronson KD, Pagani FD, Corbett JR, Murthy VL. Diagnostic accuracy of FDG PET/CT in suspected LVAD infections. *JACC Cardiovasc Imaging* 2020;**13**:1191–1202.
46. Holcman K, Małecka B, Rubiś P, Ząbek A, Szot W, Boczar K, Leśniak-Sobelga A, Hlawaty M, Wiśniowska-Śmiałek S, Stępień A, Podolec P, Kostkiewicz M. The role of 99mTc-HMPAO-labelled white blood cell scintigraphy in the diagnosis of cardiac device-related infective endocarditis. *Eur Heart J Cardiovasc Imaging* 2020; **21**:1022–1030.